Fault Diagnosis in Electric Drives using Machine Learning Approaches

Andre A. Silva*, Ali M. Bazzi†, *Member, IEEE,* Shalabh Gupta*, *Member, IEEE*

***Abstract*—This paper applies machine learning techniques to fault diagnosis in electric motor drives. As faults in motor drives can cause safety hazards in applications such as electric traction, propulsion, aircraft, and others, it is desired to diagnose the fault, i.e., detect it and isolate it, in order to recover or engage safe-mode operation. Machine learning methods are divided into three main steps: 1) Feature extraction using Principal Component Analysis (PCA); 2) Classification using the k-Nearest Neighbor (k-NN) or Probabilistic Neural Network (PNN) methods; and 3) Classifier performance evaluation using the Cross-Validation (CV) method. While electric machine, inverter, and sensor faults are introduced, the supervised learning algorithms are applied to four case studies where two fault modes occur in a current sensor, and two occur in the speed encoder. Classification accuracy, i.e., the ability to diagnose a fault, for all four cases is shown to exceed 98%. The paper also investigates a load profile used in automotive driving cycles which produces richer dynamic responses that are more interesting from an application perspective. The final goal is to implement these algorithms in real-time such that fault diagnosis can be used to isolate drive faults, especially sensor faults, and operate in a safe mode.**

I. Introduction

FAULT diagnosis is essential for early warning of incipient failures that can help in recovery of motor drive systems and in significant improvement of the remaining useful life (RUL). Machine learning approaches have been broadly studied in technical literature and have achieved successful fault detection in various applications using different methods including artificial neural networks [1]–[7]. Other approaches in the literature utilize Genetic Algorithms, Fuzzy Logic [8], [9], and Fuzzy Neural Networks [10], [11]. In this paper, we explore machine learning techniques on the sensor data of an induction motor drive system based on a model developed and experimentally validated in [12]. This paper utilizes three major steps of the machine learning approach: 1) *Feature extraction*: Principal Component Analysis (PCA) method; 2) *Classification*: the k-Nearest Neighbor (k-NN) and Probabilistic Neural Network (PNN) methods; and 3) *Classifier performance evaluation*: Cross-Validation (CV) method. While faults in the machine, power electronics, current sensors, and speed sensor are all addressed, the main goal of this paper is to diagnose sensor faults.

This paper is organized as follows. Section II presents the characteristics of the motor drive system and details the sensor data extraction procedure for different faulty conditions. Section III discusses the machine learning framework for fault diagnosis. Section IV presents the results and different case studies for fault diagnosis in the system. Finally, the paper is concluded in Section V.

* Laboratory of Intelligent Networks and Knowledge-Perception Systems (LINKS), Booth Engineering Center for Advanced Technology (BECAT), University of Connecticut, Storrs, CT.

†Advanced Power Electronics and Electric Drives Lab (APEDL), Center for Clean Energy Engineering, University of Connecticut, Storrs, CT.

II. Model Description & Data Generation

A simulation model of the motor drive similar to the one developed and experimentally verified in [12] is used for this research. The system under study is a three-phase induction motor drive shown in Fig. 1 operating under indirect field-oriented control (IFOC). The motor drive includes a 400V/100A inverter fed from a 300V dc source and connected to a 230V, four-pole, 1.5 hp induction machine.

Faults considered in the drive system are summarized in Table I and their locations are shown in Fig. 1 with red marks. Sensor faults include omission, defined as a reading of zero feedback; constant, defined as a saturated sensor; bias, defined as an offset in the sensor measurement; noise, and gain. Short circuit (SC) faults include SC to DC bus (SCDC) across an inverter IGBT, phase-to-ground fault (SCG), and phase-to-phase fault (PP) inside the machine. These are all simulated by shorting desired points through ideal switches. A broken rotor (BR) bar is simulated by varying the effective resistance of the squirrel-cage rotor. For this paper, two fault modes of each sensor are studied (SEO, SEG, CSC, and CSO). Table I describes the various possible faults in the system.

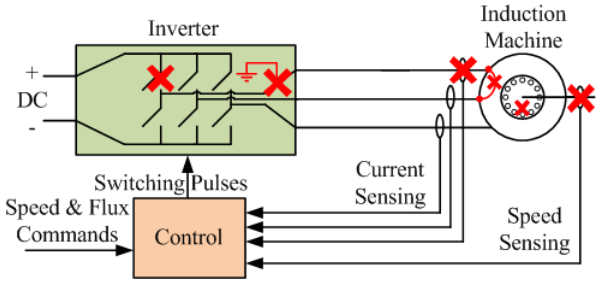

Fig. 1: Induction Motor Drive Showing Fault Locations

The Simulink model was run for 3 seconds, at a d-axis rotor flux linkage of 0.4V.s and a speed command varying in 10 uniform steps between 875 and 1750 RPM for a simple quadratic load. Once the system reaches steady-state, a fault is injected at 2 seconds (a single fault in each run). Details of data collection are shown in Table II. Data for the two control inputs (speed, d -axis rotor flux) as well as the outputs (measured speed, torque, and three-phase currents) are collected for every faulty condition in addition to the nominal condition to be used with machine learning.

978-1-4673-4974-1/13/$31.00 ©2013 IEEE

TABLE I: MOTOR FAULTS IN MAIN SUBSYSTEMS

Motor Component	Faults	Description
Speed Encoder	SEB: Speed Encoder Bias	biases the sensor output by some specific value
	SEC: Speed Encoder Constant	overrides sensor output by some specific value
	SEG: Speed Encoder Gain	amplifies sensor output by some specific gain value
	SEN: Speed Encoder Noise	sensor output with AWGN
	SEO: Speed Encoder Omission	omits the sensor output value
Current Sensors	CSB: Current Sensor Bias	biases the sensor output by some specific value
	CSC: Current Sensor Constant	overrides sensor output by some specific value
	CSG: Current Sensor Gain	amplifies sensor output by some specific gain value
	CSN: Current Sensor Noise	sensor output with AWGN
	CSO: Current Sensor Omission	omits the sensor reading value
Power Electronics	BR: Broken Rotor Bar	simulates broken rotor
	PP: Phase-to-Phase	simulates phase-to-phase fault
	SCDC: Short Circuit to DC	simulates short to DC
	SCG: Short Circuit to GND	simulates short to GND

TABLE II: DATA COLLECTED

Faults Studied	SEO, SEG, CSC, CSO
Data points per measurement	20,000
Time range	0-3 seconds
Inputs	Speed command (rpm), Rotor flux (V·sec)
Outputs	Speed (rpm), Current (A), Torque (N·m)

III. MACHINE LEARNING FRAMEWORK

The machine learning architecture used in this paper for fault diagnosis is described in Fig. 2.

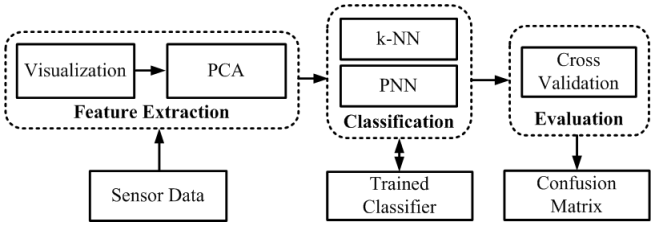

Fig. 2: Machine Learning Framework

A. Feature Extraction

The main goal of this step is data reduction by extracting a meaningful subset of data that represents the characteristics of the underlying process. This paper utilizes the PCA technique [13] that transforms the sensor data to a feature space and achieves a significant reduction in dimensionality. To apply PCA, a data set of size $n \times 1$ is partitioned into m chunks such that $p \times m = n$, where p is the length of each chunk. Then the data is arranged into a $p \times m$ matrix, denoted as X. The basic procedure for PCA is summarized as follows:

1) *Construction of Covariance Matrix:* The matrix X is processed to generate the $m \times m$ covariance matrix X_C
2) *Eigenvalue Decomposition:* This step performs the eigenvalue decomposition of X_C.
3) *Selecting Principal Components:* For data reduction, the eigenvectors corresponding to the top (e.g., three) eigenvalues with the largest magnitudes are chosen as the principal components. They are arranged in the form of an $m \times 3$ matrix V. The PCA feature space is then defined by $X_{PCA} = XV$.

B. Classification Algorithms

Two classification algorithms are discussed here k-NN and PNN.

1) k-NN: This algorithm acts as a majority vote classifier [13]. By specifying some metric as a measure of distance (typically Euclidean distance), a data point (in feature space) is assigned to a particular class according to the majority class of its k nearest neighbors. Thus, a class i is assigned to the data sample according to the probability equation $P(class = i|data\ sample) = k_i/k$, if k_i (the number of neighbors of class i), form a majority out of the k total neighbors.

2) PNN: This is a type of neural network used for classification [14]. A dataset first goes through an input layer where each point is assigned to a neuron in the hidden layer. In the hidden layer the Euclidean distance is computed of the test case from the neuron's center point, and then a radial basis function is applied. The summation layer takes in the sum of these layers per category. The decision rule for classification becomes the category with maximum value at the summation layer. Details are in [14].

C. Classifier Performance Evaluation

The performance of classifiers is evaluated using the K-fold cross validation method [13] that randomly partitions the feature data into K groups. $K-1$ groups are then used for training and the remaining group is used for testing. This process is iterated K times and the testing results are displayed in a confusion matrix. The Correct Classification Rate (CCR) is calculated from the confusion matrix by taking the sum of the diagonal entries and dividing by the sum of all entries.

IV. RESULTS

Data from the actual motor speed and phase a current is collected for the four aforementioned sensor faults and the nominal case, and used in the steps described in Section III. Results consist of the original data plots, the feature space data used to train the classifiers, and the confusion matrices for each classification technique. Finally, the CCR is calculated and used as a measure to compare the different classification algorithms. Each fault condition has $n = 20,000$ data points, e.g., $20,000$ samples of the motor speed.

A. Case Study of Speed Encoder Faults

The three classes considered here are: nominal, SEO, and SEG. The time-series of the speed sensor data are shown in Fig. 3a for the measured speed for the nominal, SEO, and SEG fault conditions at a speed command of 875 RPM.

Following the PCA procedure, the sensor data is partitioned into $m = 25$ chunks of $p = 800$ data points each. The PCA method reduced this to an 800×3 matrix such that each row represents a feature point and each column represents a

principal component or feature (PC1, PC2, and PC3). The PCA feature space with these two fault conditions and the nominal are shown in Fig. 3b. The PCA-based feature space is used to construct the classifiers. For 10-fold cross validation ($K = 10$), 720 random feature points out of the 800 are used for training, and the remaining 80 points are used for testing. This procedure is done 10 times and the classification results are averaged. The results are displayed in a confusion matrix for each classifier. Both the k-NN and the PNN classifiers achieved 100% classification as evident from the confusion matrices in Table IIIa and Table IIIb.

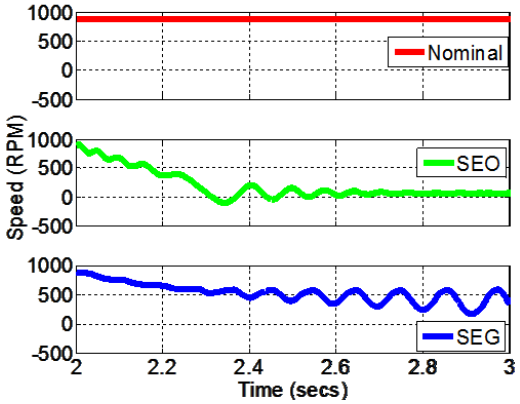

(a) Speed under the Nominal, SEO, and SEG conditions

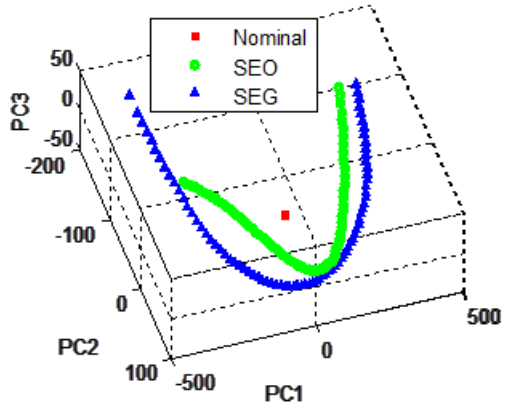

(b) PCA feature space from Fig. 3a data

Fig. 3: Visualization of Speed Faults

TABLE III: CLASSIFICATION OF SPEED FAULTS

(a) k-NN Classification of Fig. 3b data

k-NN k=1 CCR=100%		Actual Class		
		Nominal	SEO	SEG
Predicted Class	Nominal	800	0	0
	SEO	0	800	0
	SEG	0	0	800

(b) PNN Classification of Fig. 3b data

PNN spread=1.0 CCR=100%		Actual Class		
		Nominal	SEO	SEG
Predicted Class	Nominal	800	0	0
	SEO	0	800	0
	SEG	0	0	800

B. Case Study of Current Sensor Faults

A similar approach was followed for the two current sensor faults, CSC and CSO. As shown in Fig. 4a, the time-series plot of the phase-A current is not clearly separable by visual inspection; however the PCA subspace of the data achieved meaningful separation (Fig. 4b). The evaluation of these classifiers yields a 99.0% CCR for k-NN and 98.6% CCR for PNN, shown in Table IVa and Table IVb, respectively.

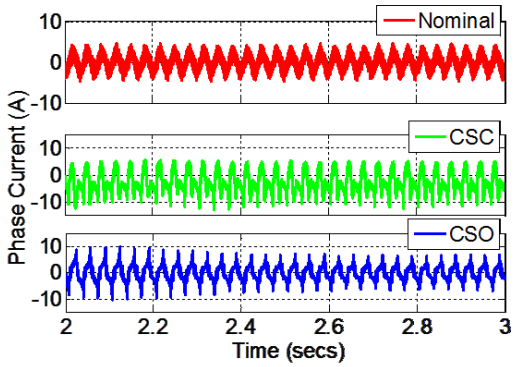

(a) Current under the Nominal, CSC, and CSO conditions

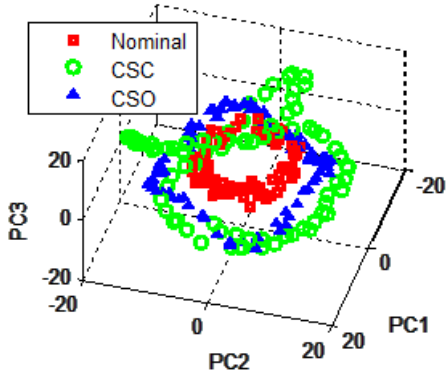

(b) PCA feature space from Fig. 4a data

Fig. 4: Visualization of Current Faults

TABLE IV: CLASSIFICATION OF CURRENT FAULTS

(a) k-NN Classification of Fig. 4b data

k-NN k=1 CCR=99.0%		Actual Class		
		Nominal	CSC	CSO
Predicted Class	Nominal	790	0	5
	CSC	0	794	4
	CSO	10	6	791

(b) PNN Classification of Fig. 4b data

PNN spread=1.0 CCR=98.6%		Actual Class		
		Nominal	CSC	CSO
Predicted Class	Nominal	777	0	0
	CSC	0	789	0
	CSO	23	11	800

C. Case Study of the complete Fault Universe

Here, all 14 faults from Table I are considered. As a pre-processing step to improve data separability, a median filter was applied prior to data analysis [15]. Following the PCA procedure, the data is partitioned into $m = 8$ chunks of length $p = 2500$. The k-NN classifier was used which achieved a CCR of 88.0%, as shown in Fig. 5.

	Nominal	BR	CSB	CSC	CSG	CSN	CSO	PP	SCDC	SCG	SEB	SEC	SEG	SEN	SEO
Nominal	1568	2	40	1	25	385	0	94	118	216	60	0	1	0	5
BR	1	2193	30	4	0	1	0	120	0	0	103	0	0	6	1
CSB	34	35	2239	11	0	55	0	29	37	29	21	0	0	2	0
CSC	2	0	2	2461	2	2	0	1	0	0	0	0	0	1	0
CSG	27	0	1	3	2323	37	0	2	48	27	27	43	5	0	3
CSN	393	3	59	1	23	1657	0	71	97	118	47	0	0	1	4
CSO	0	0	0	0	0	0	2496	0	0	0	0	0	1	3	0
PP	88	142	37	4	3	88	0	2008	29	76	47	0	0	8	0
SCDC	106	0	32	0	38	96	0	34	2103	56	8	0	8	2	0
SCG	211	0	39	3	19	130	0	80	53	1936	43	4	2	0	0
SEB	60	112	19	1	19	42	0	53	7	39	2137	0	0	5	0
SEC	0	0	0	0	43	0	0	0	0	3	0	2447	9	0	0
SEG	0	0	0	0	0	0	0	0	5	0	0	4	2474	0	0
SEN	0	8	2	7	0	1	4	6	3	0	2	0	0	2471	0
SEO	10	5	0	4	5	6	0	2	0	0	5	2	0	1	2487

Fig. 5: Confusion Matrix for all faults using k-NN (CCR=88.0%)

D. Case Study of a Driving Schedule

A speed profile of the New York City Cycle (NYCC) is scaled down to the simulated drive power level as shown in Fig. 6.

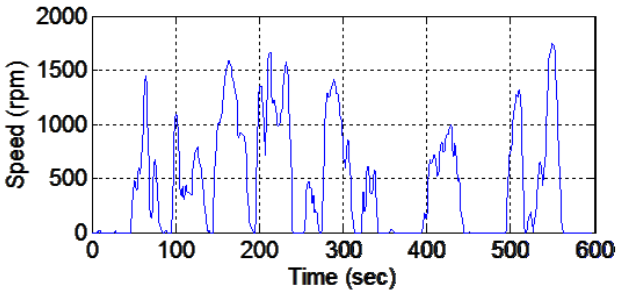

Fig. 6: NYCC drive schedule speed profile

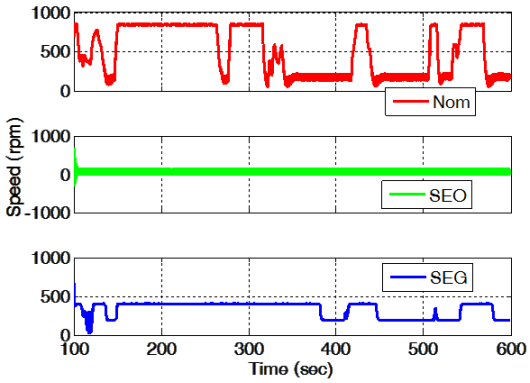

(a) Nominal, SEO, and SEG speed data for the NYCC drive cycle

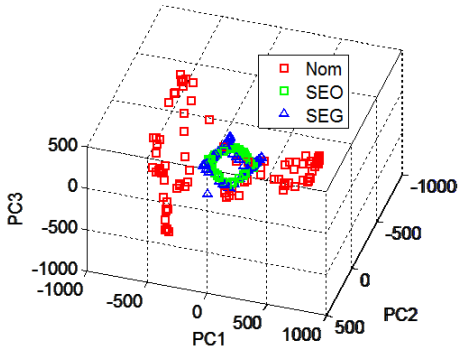

(b) PCA feature space from Fig. 7a data

Fig. 7: Visualization of Speed Faults with NYCC profile

TABLE V: Classification of Speed Faults with NYCC profile

(a) k-NN Classification of Fig. 7b data

k-NN k=1 CCR=99.4%		Actual Class		
		Nominal	SEO	SEG
Predicted Class	Nominal	2490	5	0
	SEO	0	2457	9
	SEG	0	28	2481

(b) PNN Classification of Fig. 7b data

PNN spread=1.0 CCR=99.1%		Actual Class		
		Nominal	SEO	SEG
Predicted Class	Nominal	2490	29	0
	SEO	0	2436	10
	SEG	0	25	2480

The profile is provided by the Environmental Protection Agency [16] and models urban traffic conditions of a vehicle in New York City. The drive cycle in Fig. 6 shows the motor rotational speed vs. time. Fig. 7a shows the time series for the NYCC that 598 seconds long. The faults were injected in the system at 100 seconds. The PCA produced 2490 feature points for each condition, as shown in Fig. 7b. The k-NN and PNN classifiers were evaluated using 10-fold cross validation. For each of the two classifiers, a CCR over 99% was achieved, depicted in Tables Va and Vb.

Overall, our goal is to implement these algorithms online such that fault identification can be used to isolate sensor faults and operate in an open-loop mode as proposed in Fig. 8. This scenario would be similar to an electric vehicle having a chance to drive a short distance and park safely under hazardous sensor faults.

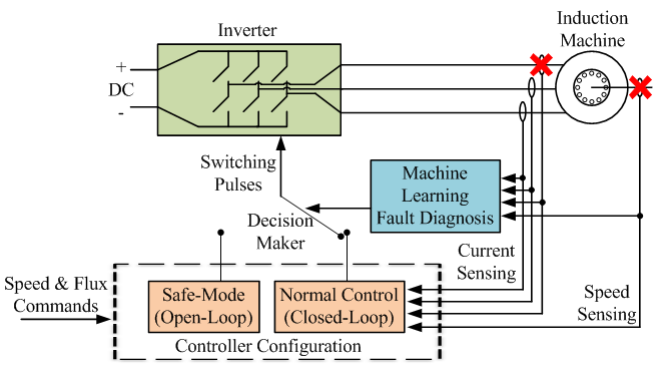

Fig. 8: Proposed real-time fault detection method

V. Conclusion

This paper expands the application of machine learning techniques to fault diagnosis in electric motor drives. We performed two main algorithms, k-NN and PNN and achieved classification accuracy exceeding 98% of current and speed sensor faults. The paper also performed fault diagnosis while using a real-world driving profile such as the NYCC schedule. The computation time of the classifiers, once trained, is of the order of a few seconds. Future work would involve online implementation of the classifiers, and testing on a real-world experimental test-bed.

References

[1] R. Schoen, B. Lin, T. Habetler, J. Schlag, and S. Farag, "An unsupervised, on-line system for induction motor fault detection using stator current monitoring," *IEEE Transactions on Industry Applications*, vol. 31, no. 6, pp. 1280–1286, Nov/Dec 1995.

[2] Y. Murphey, M. Masrur, Z. Chen, and B. Zhang, "Model-based fault diagnosis in electric drives using machine learning," *IEEE/ASME Transactions on Mechatronics*, vol. 11, no. 3, pp. 290–303, June 2006.

[3] Y. Murphey, J. Park, Z. Chen, M. Kuang, M. Masrur, and A. Phillips, "Intelligent hybrid vehicle power control part i: Machine learning of optimal vehicle power," *IEEE Transactions on Vehicular Technology*, vol. 61, no. 8, pp. 3519–3530, Oct. 2012.

[4] Y. Murphey, J. Park, L. Kiliaris, M. Kuang, M. Masrur, A. Phillips, and Q. Wang, "Intelligent hybrid vehicle power control part ii: Online intelligent energy management," *IEEE Transactions on Vehicular Technology*, vol. 62, no. 1, pp. 69–79, Jan. 2013.

[5] S. Ho and K. Lau, "Detection of faults in induction motors using artificial neural networks," in *Seventh International Conference on Electrical Machines and Drives*, no. 412, Sep 1995, pp. 176 –181.

[6] S. Premrudeepreechacharn, T. Utthiyoung, K. Kruepengkul, and P. Puongkaew, "Induction motor fault detection and diagnosis using supervised and unsupervised neural networks," in *IEEE International Conference on Industrial Technology*, vol. 1, 2002, pp. 93 – 96.

[7] J. Martins, V. Pires, and A. Pires, "Unsupervised neural-network-based algorithm for an on-line diagnosis of three-phase induction motor stator fault," *IEEE Transactions on Industrial Electronics*, vol. 54, no. 1, pp. 259 –264, Feb. 2007.

[8] F. Filippetti, G. Franceschini, C. Tassoni, and P. Vas, "Recent developments of induction motor drives fault diagnosis using ai techniques," *IEEE Transactions on Industrial Electronics*, vol. 47, no. 5, pp. 994 –1004, Oct 2000.

[9] A. Siddique, G. Yadava, and B. Singh, "Applications of artificial intelligence techniques for induction machine stator fault diagnostics: review," in *4th IEEE International Symposium on Diagnostics for Electric Machines, Power Electronics and Drives*, Aug. 2003, pp. 29 – 34.

[10] S. Zhang, T. Asakura, X. Xu, and B. Xu, "Fault diagnosis system for rotary machines based on fuzzy neural networks," in *IEEE/ASME International Conference on Advanced Intelligent Mechatronic*, vol. 1, July 2003, pp. 199 – 204.

[11] Y. Ivonne, D. Sun, and Y. He, "Fault diagnosis using neural-fuzzy technique based on the simulation results of stator faults for a three-phase induction motor drive system," in *Proceedings of the Eighth International Conference on Electrical Machines and Systems*, vol. 3, Sept. 2005, pp. 1966 –1971.

[12] A. Bazzi, A. Dominguez-Garcia, and P. Krein, "Markov reliability modeling for induction motor drives under field-oriented control," *IEEE Transactions on Power Electronics*, vol. 27, no. 2, pp. 534–546, Feb. 2012.

[13] C. M. Bishop, *Pattern Recognition and Machine Learning*. New York: Springer, 2006.

[14] R. O. Duda, P. E. Hart, and D. G. Stork, *Pattern Classification*, 2nd ed. New York: Wiley-Interscience Publication, 2001.

[15] A. Bazzi and P. Krein, "Utilization of median filters in power electronics: Traction drive applications," in *Proc. IEEE Applied Power Electronics Conference*, 2013, in Press.

[16] [Online]. Available: http://www.epa.gov/nvfel/testing/dynamometer.htm